Monoclonal antibody to a DNA-binding domain of p53 mimics charge structure of DNA: anti-idiotypes to the anti-p53 antibody are anti-DNA

Johannes Herkel[1], Na'aman Kam[2], Neta Erez[3], Avishai Mimran[2], Alexander Heifetz[4], Miriam Eisenstein[5], Varda Rotter[3] and Irun R. Cohen[2]

[1] Department of Medicine, Johannes Gutenberg University, Mainz, Germany
[2] Department of Immunology, The Weizmann Institute of Science, Rehovot, Israel
[3] Department of Molecular Cell Biology, The Weizmann Institute of Science, Rehovot, Israel
[4] Department of Biological Chemistry, The Weizmann Institute of Science, Rehovot, Israel
[5] Department of Chemical Services, The Weizmann Institute of Science, Rehovot, Israel

Antibodies to DNA are important markers of various autoimmune diseases and can be pathogenic; however, their generation is not understood. We previously reported that anti-DNA antibodies could be induced in mice by idiotypic immunization to PAb-421, an antibody to a DNA-binding domain of p53. We now report that two monoclonal antibodies of moderate affinity ($K_D \asymp 10^{-7}$), raised from PAb-421-immunized mice, specifically recognized both PAb-421 and DNA. These antibodies feature multiple arginine residues in the antigen-binding site, a unique characteristic of disease-associated anti-DNA antibodies; nevertheless, these anti-DNA antibodies show specific complementarity to PAb-421 by competing with p53 for PAb-421 binding and recognize defined oligonucleotides with a specificity similar to that of p53. To study the structural basis for the cross-recognition of PAb-421 and DNA by the anti-DNA antibodies, we constructed computer models (fine-tuned by protein-protein docking) of PAb-421 and one of the monoclonal anti-DNA antibodies. The modeled structures manifested structural complementarity. Most notably, the modeled structure of PAb-421 resembled the structure of DNA by the positions of negatively charged groups and aromatic side chains. Thus, a protein molecule may mimic the structure of DNA and the elusive generation of anti-DNA antibodies could be explained by idiotypic immunity to a DNA-binding protein, like p53.

Received	15/6/04
Revised	1/9/04
Accepted	14/9/04

Key words: Autoantibodies / Anti-DNA / p53 / Structural mimicry/structure modeling

1 Introduction

Antibodies to DNA are serological markers of various autoimmune diseases, including systemic lupus erythematosus (SLE) [1] and autoimmune hepatitis (AIH) [2], and at least some anti-DNA antibodies can be pathogenic [1]. However, the generation of anti-DNA antibodies is difficult to explain: native DNA itself is poorly immunogenic and cannot drive anti-DNA immunity [3]. Nevertheless, the autoimmune response to DNA clearly has features indicative of being antigen-driven in IgG isotype and affinity maturation [4]. To account for autoimmunity to DNA, we hypothesized that an immune response to proteins that mimic the structure of DNA might drive the generation of anti-DNA antibodies. Indeed, an antibody resembling DNA could be generated by an immune response to a DNA-binding domain [5] by way of idiotypic mimicry [6, 7]. The idea is that in order to be recognized by a DNA-binding domain, both DNA and an antibody to the DNA-binding domain must have some degree of structural similarity. Thus, immunity to a DNA-binding protein may induce an antibody resembling DNA, and such a DNA-mimicking antibody may induce anti-idiotypes that are anti-DNA. To test this possibility, we used the p53 molecule as a prototypic DNA-binding protein, and we studied a prototypic monoclonal antibody that reacts with the C-terminal DNA-binding domain of p53, PAb-421.

The p53 tumor-suppressor molecule plays a central role in the cellular response to DNA damage [8], and its C-terminal domain was shown to recognize various types of damaged DNA [9–11]. The C terminus of p53, besides binding DNA, also reacts with the monoclonal antibody PAb-421 [12]. Thus, PAb-421 may structurally resemble what is recognized by p53 as damaged DNA. If this is the case, then immunization with PAb-421 might induce anti-

[DOI 10.1002/eji.200425371]

Abbreviations: AIH: Autoimmune hepatitis **CDR:** Complementarity determining region **PDB:** Protein data bank

idiotypes that function as an image of the p53 DNA-binding domain, and would thus react both with PAb-421 and with DNA.

Indeed, we previously reported that immunization of mice with PAb-421 induced the formation of anti-idiotypic antibodies that also bind DNA [5]. Moreover, sera of SLE patients contain antibodies to the DNA-binding domain of p53 and antibodies that bind both PAb-421 and DNA [13]. Recently, we reported that the presence of anti-DNA antibodies in the sera of AIH patients is associated with the presence of antibodies to the p53 DNA-binding domain [14]. Thus, immunity to DNA in mice and in human patients with SLE or AIH may be driven by idiotypic immunity to a protein with a DNA-binding domain like that of p53.

We raised two monoclonal antibodies, designated Idi-1 and Idi-2, generated by immunization with PAb-421 [5]. These monoclonal anti-idiotypic antibodies reacted specifically with PAb-421 and DNA [5]. The aims of the present study were to probe the functional complementarity of PAb-421 and DNA on the one hand and of the monoclonal anti-idiotypes and p53 on the other hand, and to test, by molecular modeling, whether the combining site of PAb-421 might manifest structural features shared with DNA. The results provide a structural basis for the observed immunological cross-reactivity of the monoclonal anti-idiotypes to antibody PAb-421 and to DNA.

2 Results

2.1 Monoclonal antibodies bind DNA and PAb-421

We demonstrated previously that the monoclonal antibodies Idi-1 and Idi-2 can specifically bind both PAb-421 and DNA, single- or double-stranded [5]. To exclude the possibility that DNA binding might be due to complexing of the antibody with a DNA-binding protein from the hybridoma supernatant [15], we compared the binding properties of Idi-1 and Idi-2, purified under non-dissociating or dissociating conditions (Fig. 1). The binding properties of the antibodies were similar under both conditions. Moreover, the amount of both Idi-1 (A) and Idi-2 (B) needed for half-maximal binding of single-stranded DNA was lower than that needed for binding double-stranded DNA or PAb-421, indicating a binding preference for single-stranded DNA with an apparent tentative K_D in the range of 10^{-7}. In addition to DNA bound to a solid-phase, both antibodies recognized soluble DNA, as indicated by the concentration-dependent inhibition of reactivity in ELISA to matrix-bound single-stranded DNA by soluble single-stranded DNA (Fig. 1C).

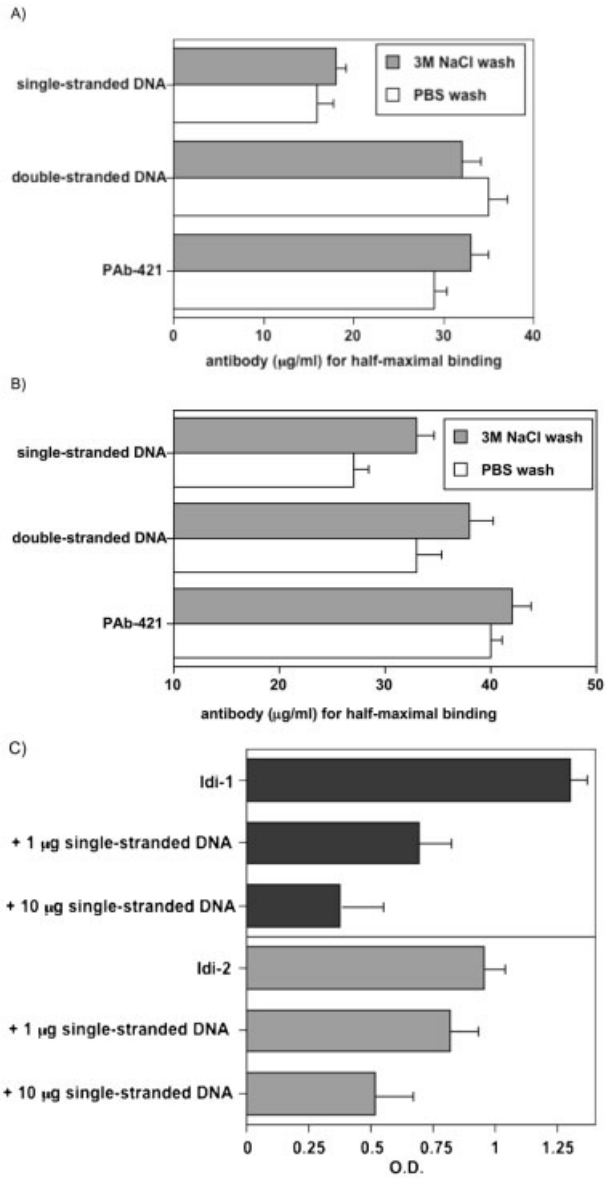

Fig. 1. Idi-1 and Idi-2 bind DNA, single- or double-stranded, and PAb-421. The monoclonal antibodies Idi-1 (A) and Idi-2 (B), purified under dissociating conditions (3 M NaCl wash) or non-dissociating conditions (PBS wash), were assessed by ELISA for binding to single-stranded DNA, double-stranded DNA, or PAb-421 in serial dilutions. The antibody concentration producing half-maximal binding ± SD is shown. Both antibodies bind preferentially to single-stranded DNA. Binding of 10 μg antibody to single-stranded DNA assessed by ELISA (C) was dose-dependently inhibitable by addition of soluble single-stranded DNA (1 or 10 μg; $p<0.016$).

2.2 Idi-1 and Idi-2 compete with p53 for PAb-421-binding

Because both antibodies could specifically bind both PAb-421 and DNA, single- or double-stranded, Idi-1 and Idi-2 seemed to mimic the p53 DNA-binding domain functionally. To confirm the complementarity of Idi-1 and Idi-2 to PAb-421, we performed an immunoprecipitation assay (Fig. 2A). Equal amounts of total extracts of cells over-expressing mutant p53, metabolically labeled with [^{35}S]methionine, were immunoprecipitated with equal amounts of PAb-421 in the presence of increasing amounts of Idi-1 or Idi-2. Both Idi-1 and Idi-2 could compete with p53 and inhibit its binding to PAb-421.

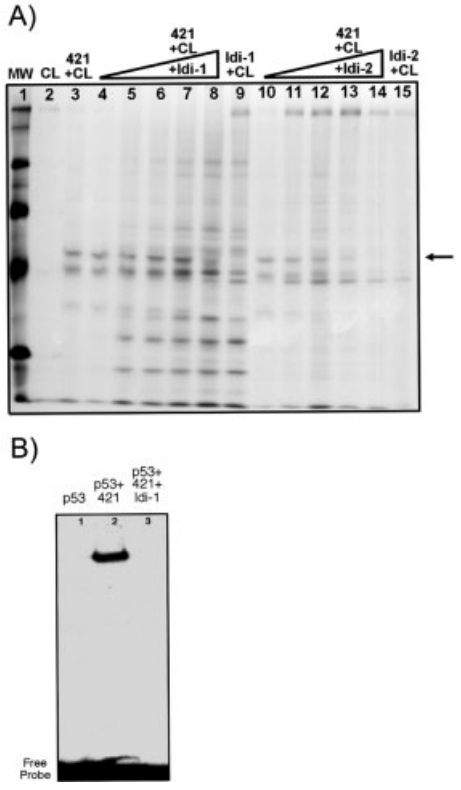

Fig. 2. Idi-1 and Idi-2 compete with p53 for PAb-421 binding. (A) Idi-1 and Idi-2 inhibit the binding of p53 to PAb-421: MethA cell lysates as a source of p53 were immunoprecipitated by PAb-421. To this reaction, we added increasing amounts (1, 5, 10, 20 and 50 μg) of Idi-1 (lanes 4–8) or Idi-2 (lanes 10–14). The arrow points at the position of p53. A molecular weight marker is indicated at the left (lane 1, MW). The p53 in the cell lysate (CL) itself did not precipitate (lane 2), unless PAb-421 was added (lane 3). Lanes 9 and 15 are a control with 50 μg of the antibodies without PAb-421. Note that increasing amounts of Idi-1 or Idi-2 decreased the amounts of precipitated p53. (B) Idi-1 inhibits the activation of p53 by PAb-421. The p53-responsive element was used as the probe in a band shift assay. Recombinant p53 produced by bacteria cannot bind the responsive element spontaneously (lane 1) unless PAb-421 is added (lane 2). One microliter of PAb-421 from ascites fluid was added to each reaction to activate p53. Note that the addition of 3 μg of purified Idi-1 (lane 3) totally abolished the activation of p53 by the PAb-421 antibody.

However, it is known that PAb-421 also can precipitate other proteins from cell lysates [16], probably those with DNA-binding domains similar to that of p53; the p53 band in Fig. 2A is marked by an arrow. To exclude the possibility that DNA-binding proteins in the cell lysate other than p53 may have a non-specific influence on the binding of PAb-421 to p53, Idi-1 or Idi-2, we also probed the competition of Idi-1 and Idi-2 with p53 for PAb-421-binding in a band-shift analysis (Fig. 2B). It was shown previously that recombinant p53 produced in bacteria does not bind spontaneously to the p53-responsive element oligonucleotide (lane 1), and that PAb-421 binding to the p53 C-terminal epitope activates the p53 molecule and enables its central DNA binding domain to bind the responsive element probe (lane 2) [17]. Addition of Idi-1 (lane 3) completely abolished the PAb-421-induced binding of p53 to the responsive element probe. Idi-2 also inhibited p53 binding to the responsive element (not shown). Thus, both Idi-1 and Idi-2 anti-idiotypic antibodies can compete with p53 for PAb-421 binding.

2.3 Idi-1 and Idi-2 mimic p53 in binding to specific DNA oligonucleotides

We have shown that Idi-1 and Idi-2 specifically bound both single- or double-stranded DNA and that DNA-binding was increased when the DNA was damaged by γ-irradiation [5]. These binding preferences are similar to those of p53; it has been shown that the C terminus of p53 can bind various types of DNA, including damaged DNA [9–11]. To confirm that p53, Idi-1 and Idi-2 bind DNA with similar specificity, we compared the binding of p53, Idi-1 and Idi-2 to defined oligonucleotides. We synthesized four 20-mers, oligo dA, oligo dC, oligo dT and oligo dG, and performed a band-shift analysis in which the two antibodies and the p53 protein interacted with each of the four oligomers. Fig. 3A shows that the binding of the p53 protein and the two antibodies were similar: all three proteins bound only to oligo dG and not to the other three oligonucleotides.

To further characterize the binding to oligo dG, we tested whether the recognition requires G at the ends of the oligonucleotide chain, or whether a G-rich sequence can be recognized in the body of the DNA sequence. We tested two oligonucleotides: dG_{16} with two dT residues at each end ($dT_2dG_{16}dT_2$) and dT_{16} with two dG residues at

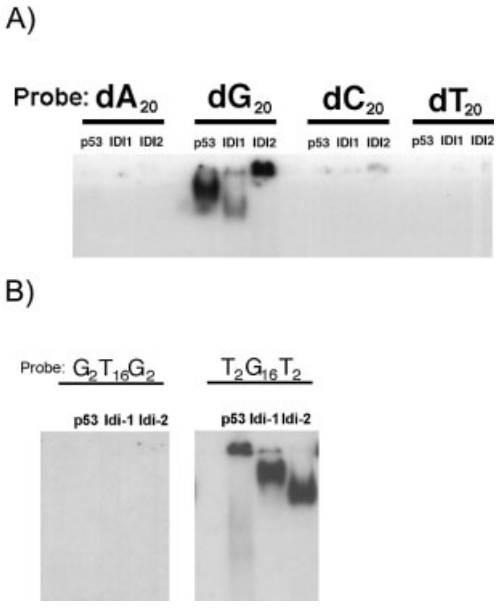

Fig. 3. Binding of synthetic oligonucleotides by p53 and antibodies. (A) Four 20-mer oligonucleotides, poly dA, poly dG, poly dT, and poly dC, were used as probes to test the DNA binding specificities of p53 and the two antibodies. Each oligonucleotide was added to a binding reaction with 4 μg of Idi-1 or Idi-2, and 2 μl of a recombinant p53 lysate. The reactions were loaded on a native gel, including a free probe lane for each oligonucleotide. (B) Two probes, $dG_2dT_{16}dG_2$ and $dT_2dG_{16}dT_2$, were used as in A, to further characterize the binding specificities of the antibodies and p53 to dG residues.

each end ($dG_2dT_{16}dG_2$). Fig. 3B shows that both the antibodies and the p53 protein bound to the G-rich $dT_2dG_{16}dT_2$ sequence and not to the $dG_2dT_{16}dG_2$ sequence. Thus, both Idi-1 and Idi-2 antibodies mimic p53 in recognizing specifically dG-rich DNA motifs in which the terminal two residues need not be dG.

2.4 CDR sequences of Idi-1 and Idi-2

The above results indicated that Idi-1 and Idi-2 did in fact bind to ligands to which p53 itself could bind. This raised the question of whether the antigen-binding sites of Idi-1 and Idi-2 might have sequence homology to p53. The variable regions of Idi-1 and Idi-2 were sequenced (Fig. 4) and the complementarity determining regions (CDR) of both antibodies were compared to p53. Neither CDR sequences showed any significant homology to p53. This suggests that the ability of p53 and the antibodies to bind the same ligand is based on structural complementarity fashioned by different amino acid sequences.

We then compared the variable region sequences of Idi-1 and Idi-2 with that of other anti-DNA antibodies. Over 250 sequences of anti-DNA antibodies from autoimmune mice and from patients with SLE have been determined. Even though the primary structure of anti-DNA antibodies is highly diverse, it has been noted that positively charged arginine side chains play an important role in DNA binding [18]. Previous work on anti-DNA antibodies indicated that

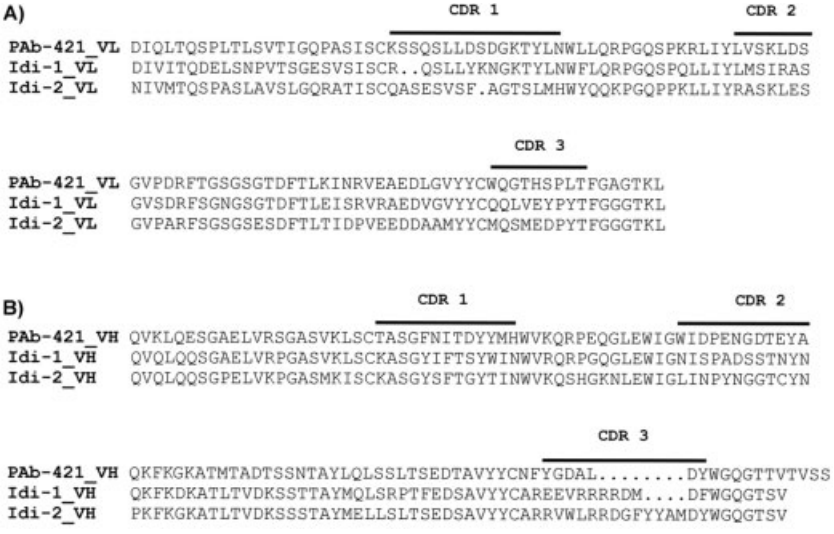

Fig. 4. Amino acid sequences of the variable regions of PAb-421, Idi-1 and Idi-2. Complementarity determining regions (CDR) of the light chain (A) or of the heavy chain (B) are aligned. Note the arginine residues in the heavy chain CDR3 regions of Idi-1 and Idi-2, typical of anti-DNA antibodies.

arginines in VH positions 100 and 100A (Kabat numbering scheme) are important for DNA binding [4, 19, 20].

Interestingly, sequence analysis of Idi-1 and Idi-2 showed an enriched arginine content in CDR-H3 (Fig. 4): Idi-1 contains four arginine residues in CDR-H3, including two consecutive arginines in VH positions 100 and 100A. The CDR-H3 of Idi-2 was found to contain three arginines, including two consecutive arginine residues in VH positions 99 and 100. Although there was no homology between the Idi-1 and Idi-2 anti-idiotypic antibodies and p53 at the amino acid sequence level, both antibodies manifest the characteristic arginine motifs of anti-DNA antibodies associated with SLE.

2.5 Model structures of PAb-421 and Idi-1

To explore the structural basis for the functional cross-recognition of PAb-421 and DNA by Idi-1 and Idi-2, we modeled the structures of PAb-421 and Idi-1 based on their variable region amino acid sequences (Fig. 4). This procedure has been shown to generate useful approximations of the variable region crystal structure [21]. Here, we further optimized the model structures by docking the recognition sites of PAb-421 and Idi-1 and manual editing to eliminate clashes by allowing for small positional rotations. Idi-1 was preferable to Idi-2 because of a shorter H3 loop, which allowed more accurate modeling. The model structures of the two antibodies are shown in Fig. 5. The antigen recognition site of PAb-421 (Fig. 5; left panel) has a deep groove resulting from the relatively short CDR3 loops in the light and heavy chains and the long CDR1 loops. The most prominent feature of the antigen-binding site of Idi-1 (Fig. 5; right panel) is a ridge, formed from the long CDR1 loop in the light chain (L1) and the CDR3 loop in the heavy chain (H3). Thus, PAb-421 and Idi-1 show geometric complementarity.

2.6 Charge distribution of the PAb-421 and Idi-1 model structures

The electrostatic potential on the surfaces of both molecules (Fig. 6A; upper panel: top view on combining sites; lower panel: side view on combining sites) displays large patches, negative for PAb-421 (left panel) and positive for Idi-1 (right panel). Therefore, PAb-421 and Idi-1 show complementarity also by electrostatic potential. The occurrence of well-defined electrostatic patches is advantageous for geometric-electrostatic docking [22].

We noted that the distribution of negatively charged residues in the PAb-421 variable region manifests a remarkable spatial correspondence to the positions of negatively charged phosphate groups in B-DNA. Fig. 6B shows a space filling representation of PAb-421 in which the negative groups of aspartate and glutamate side chains are highlighted in red (left). The negatively charged residues of the PAb-421 variable region are positioned similar to the negatively charged phosphate groups in DNA: on the right of Fig. 6B, B-DNA (cyan) with the phosphate groups highlighted in magenta is superimposed onto the PAb-421 variable region; for better

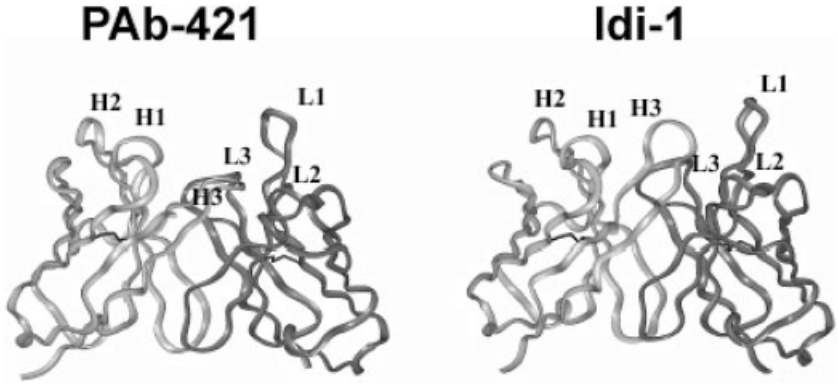

Fig. 5. Structural models of PAb-421 and Idi-1. Model structures of PAb-421 and Idi-1 were obtained for each antibody separately based on structures of antibodies from the Protein data bank (PDB). The models were then optimized by docking the Fv domains of the two model structures to obtain a model structure of the Fv-Fv complex; only those docking models were considered further that were based on interactions between the CDR of the two antibodies. Finally, the conformations of side chains of the interacting CDR were manually modified to eliminate clashes and to optimize the interactions. Shown are the ribbon diagrams of the final model structures of PAb-421 (left) and Idi-1 (right), which have excellent geometric and electrostatic complementarity. The light chains are depicted in dark gray and the heavy chains are depicted in light gray. The CDR loops are indicated. Note the long L1 and H1 and the short L3 and H3 of PAb-421, forming a groove in the binding site.

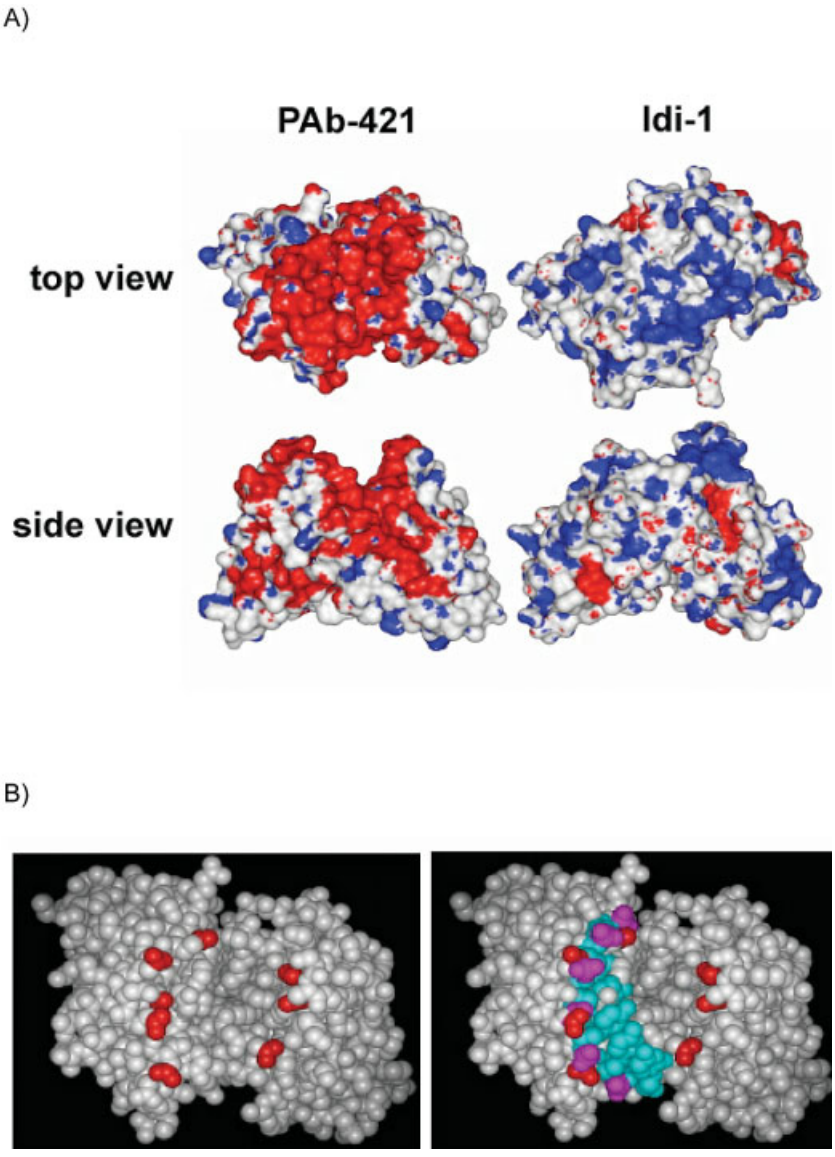

Fig. 6. Charge distribution of the PAb-421 and Idi-1 model structures. (A) Top view (top) and side view (bottom) of the combining sites of the two antibodies. The solvent accessible surfaces of PAb-421 (left) and Idi-1 (right) are colored according to the electrostatic potential. The surface is red where the potential is less than –3kT/e and blue where the electrostatic potential exceeds +3kT/e. Note the groove in the recognition site of PAb-421 and the ridge in the recognition site of Idi-1. (B) Space filling representation of PAb-421, in which the negative groups of aspartate and glutamate side chains are emphasized in red (left). On the right we present a superposition of a single B-DNA strand (cyan) onto the recognition site of PAb-421 (view from top); the negative phosphate groups of the DNA are emphasized in magenta. Note that the positions of four negative side chains of PAb-421 correspond spatially to four phosphate groups in B-DNA.

visualization, just a single DNA strand is shown. Both structures, B-DNA and PAb-421 show a remarkable spatial correspondence of the negative charges. In addition, the groove in the binding site of PAb-421 is lined with many aromatic side chains, which resemble the aromatic nature of purine and pyrimidine bases. Thus, the combining site of PAb-421 appears to imitate the distribution of charges and aromatic groups in B-DNA.

2.7 Docking model of the complex between PAb-421 and Idi-1

The best solution produced by the rotation-translation docking scan (Fig. 7) has an exceptionally high geometric-electrostatic complementarity score and a high statistical significance (5.3 standard deviations). The interactions between the modeled antibodies involve

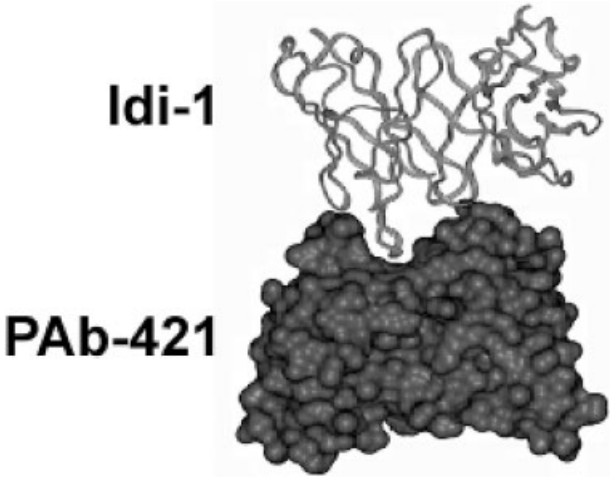

Fig. 7. Interaction model of PAb-421 and Idi-1. Docking model (side view) of PAb-421 (dark gray, bottom) and Idi-1 (light gray, top) showing that the CDR1 and CDR3 loops of IDI-1 interact with the groove in the antigen recognition site of PAb-421.

only their CDR. Thus, the ridge formed by L1 and H3 of Idi-1 interacts with the groove in the binding site of PAb-421. Tight contacts are formed between the positive arginine and lysine side chains of Idi-1 and negative and aromatic side chains of PAb-421; the CDR-CDR contact residues of up to 5 Å are listed in Table 1. The docking program MolFit treats the molecules as rigid bodies and tolerates small penetrations of one molecule into the other. Hence, the docking can only produce an approximate structure of the complex, in particular when two modeled structures are docked [23]. Nevertheless, the excellent geometric and electrostatic complementarity displayed by the docking model supports the independently formed models of the individual antibody combining sites.

Table 1. CDR-CDR contact residues of Idi-1 and PAb-421 model structures

Idi-1	PAb-421
L-30 (L1)	D-33 & K-35 (L1), Y-37 (L1)
Y-31 (L1)	Y-33 (H1), D-52 (H2)
K-32 (L1)	D-31 (L1), L-55 (L2), G-100 (H3), D-101(H3)
N-33 (L1)	D-31 (L1), G-96 (L3), T-97 (L3)
N-33 (L1)	S-99 (L3)
G-34 (L1)	D-31 (L1), D-33 (L1)
K-35 (L1)	S-32 (L1), D-33 (L1)
T-36 (L1)	D-33 (L1)
V-97 (L3)	E-54 (H2)
E-98 (L3)	D-31 (H1), E-54 (H2)
Y-99 (L3)	T-30 (H1), D-31 (H1)
W-33 (H1)	N-55 (H2)
V-101 (H3)	N-55 (H2)
R-102 (H3)	N-55 (H2), D-57 (H2)
R-104 (H3)	E-54 (H2)
R-105 (H3)	D-52 (H2), E-54 (H2)

3 Discussion

The results presented here describe functional and structural properties of monoclonal anti-DNA antibodies that were generated not by poorly immunogenic DNA, but by idiotypic immunization to a prototypic monoclonal antibody, PAb-421, which binds the C-terminal DNA-binding domain of p53. The two monoclonal anti-PAb-421 antibodies, Idi-1 and Idi-2, seem to mimic the function and structure of the C-terminal p53 DNA-binding domain. Both Idi-1 and Idi-2 could specifically compete with p53 for binding to PAb-421 (Fig. 2). Additionally, both antibodies bind DNA, double- and single-stranded (Fig. 1), and the binding to single-stranded DNA is enhanced following γ-irradiation [5]; this, too, is similar to p53 [9–11]. Moreover, in gel-shift assays performed with defined oligonucleotide probes, both p53 and the two anti-idiotypic antibodies bound preferentially dG-rich sequences (Fig. 3). Thus, p53 and the Idi-1 and Idi-2 antibodies recognize not merely damaged DNA, but a more defined sequence motif enriched in dG, but in which the terminal two residues need not be dG. Our results suggest that damaged DNA recognized by p53 and by the Idi-1 and Idi-2 antibodies has a chemically defined structure. To verify this hypothesis, we plan to perform a more detailed analysis of the fine specificities of the nucleotide motifs recognized as damaged DNA by p53.

To learn whether the functional mimicry between Idi-1, Idi-2 and p53 is also evident at the amino acid level, we sequenced the CDR domains of both monoclonal antibodies (Fig. 4). Comparison of the amino acid sequences to the C terminus of p53 revealed no similarity. However, the binding of a ligand by an antibody depends on structural complementarity. In other words, the functional mimicry between p53 and the antibodies requires similarity at the structural level, and not necessarily at the level of the primary sequence. Note that the C-terminal DNA-binding domain of p53 does not seem to have a stable structure when crystallized; this implies that the carboxy domain can assume several

conformations [24]. Presumably, the different conformations allow the domain some flexibility in ligand binding. The antibodies described here may provide an immunological approach to the structure of at least one of the functional conformations of the flexible C-terminal domain of p53.

Although the antibodies have no sequence homology to p53, Idi-1 and Idi-2 do manifest a characteristic feature of the anti-DNA antibodies isolated from SLE patients: multiple arginine residues in the CDR3 region of the heavy chain (Fig. 4). In this regard, Idi-1 and Idi-2 seem to be indistinguishable from the anti-DNA antibodies associated with SLE or AIH; however, their affinity seems to be considerably lower. Previously, we reported that MRL/MpJ-Fas^{lpr} mice, which spontaneously develop murine lupus, spontaneously produced antibodies that bind to both PAb-421 and DNA. These mice also produced antibodies that bound to p53 [5]. Anti-DNA antibodies that cross-react with PAb-421 were detected in sera taken from human SLE patients [13] and AIH patients [14]. Thus, anti-DNA antibodies that also recognize PAb-421 are not a laboratory artifact.

To explore the structural basis for the cross-recognition of DNA and PAb-421 by p53 and by antibody Idi-1, we modeled the structures of the PAb-421 and Idi-1 Fv domains (Fig. 5); modeling can generate useful approximations of the variable region crystal structure [21]. Although computer modeling is not a definitive determination of molecular structure, the models reported here are not arbitrary: (1) the variable regions interact only by way of their CDR, five of which have well-studied canonical structures; (2) the modeled molecules are highly complementary, both by electrostatic potential (Fig. 6) and by geometric fit (Figs. 5 and 7), and (3) the models are restrained and refined by mutual docking. Most intriguing was the finding that the model structure of PAb-421 manifests a remarkable structural similarity to DNA; notably in the spatial distribution of charges along with aromatic moieties (Fig. 6B): The positions of negatively charged amino acids in the PAb-421 combining site correspond to the positions of the negatively charged phosphate groups in B-DNA. In addition, the groove of the PAb-421 binding site is lined with aromatic side chains reminiscent of the aromatic purine and pyrimidine bases. The complementarity of Idi-1 to the PAb-421 model would explain its cross-reactivity to DNA; tight contacts are formed between the positive arginine and lysine side chains of Idi-1 and the negative and aromatic side chains of PAb-421 and thus to DNA (Fig. 7; Table 1). This exercise in modeling is entirely consistent with the fact that immunization to PAb-421 did indeed induce anti-DNA.

Thus, p53 and the PAb-421 anti-p53 antibody may be considered as a prototypic DNA-binding molecule and a related prototypic DNA-mimicking antibody. In SLE or AIH, other DNA-binding molecules, like histones [25], may also induce idiotypic immunity to DNA-binding domains and to DNA. Indeed, idiotypic molecular mimicry of DNA may explain the spreading of autoimmunity to a variety of DNA- and RNA-binding proteins both in SLE and in AIH; immunization of mice to PAb-421 not only induced antibodies to p53 but also to histones [5].

4 Materials and methods

4.1 Anti-PAb-421 antibodies

The monoclonal anti-PAb-421 antibodies Idi-1 and Idi-2 were generated as described [5]. Briefly, BALB/c mice were immunized three times with PAb-421 and the spleen cells of the mouse that produced the highest anti-PAb-421 titers were fused with NSO myeloma cells. Supernatants of the growing cells were screened by ELISA for binding to PAb-421 and to DNA. The hybridomas Idi-1 and Idi-2 were isolated and cloned twice by limiting dilution. Antibodies were purified from hybridoma supernatants by ammoniumsulfate precipitation and Protein G chromatography. To exclude the possibility that other proteins, attached to Idi-1 and Idi-2 mediated the binding to DNA [15], we extensively washed the Protein G-bound antibody with 3 M NaCl before acid-elution; nevertheless, these antibody preparations specifically bound DNA (Fig. 1). Serial dilutions of purified antibodies, with or without 3 M NaCl wash, were tested for DNA and PAb-421 binding by ELISA as described [5], and the amount of antibody producing half-maximal binding was assessed to estimate the binding preferences.

4.2 Immunoprecipitation

Meth-A cells, which overexpress p53 [26], were metabolically labeled for 1 h at 37°C in methionine-free Dulbeco's modified Eagle's medium supplemented with 10% heat-inactivated fetal calf serum and 0.125 mCi/ml of [^{35}S]methionine (APBiotech, Freiburg, Germany). The cells were lysed in PLB buffer containing 10 mM phosphate buffer pH 7.5, 100 mM NaCl, 1% Triton, 0.5% sodium deoxychalate, and 0.1% SDS, and precleared on 50% protein A-Sepharose CL-4B (Sigma). Equal amounts of labeled cells were incubated overnight at 4°C with 1 µl PAb-421 ascites fluid and increasing amounts of affinity purified Idi-1 or Idi-2 antibodies. Immune complexes were precipitated by incubation with protein A-Sepharose CL-4B for 2 hr at 4°C in a slurry, followed by three washes with PLB. Immunoprecipitates were separated on 10% polyacrylamide-SDS gels.

4.3 Band-shift analysis

Six 20-mer oligonucleotides and the p53 responsive element were synthesized for use as probes in band-shift analyses: 5′-AAAAAAAAAAAAAAAAAAAA-3′; 5′-CCCCCCCCCCCC-CCCCCCCC-3′; 5′-TTTTTTTTTTTTTTTTTTTT-3′; 5′-GGGG-GGGGGGGGGGGGGGGG-3′; 5′-TTGGGGGGGGGGGGGG-GGGTT-3′; 5′-GGTTTTTTTTTTTTTTTTGG-3′. The double-strand p53 responsive element is: 5′- TCGAGAGGCATGTC-TAGGCATGTCTC-3′ and its complementary strand. For double-strand probes, the two strands were first incubated at 70°C for 4 min, and then were cooled slowly to room temperature before labeling. Oligonucleotides were end-labeled by the T4 polynucleotide kinase (PNK; New England Biolabs, Hertfordshire, UK), with ^{32}P (APBiotech). The 10 μl reaction included 100 ng of the DNA probe, 50 μCi of ^{32}P, 1×PNK buffer and 10 U of PNK. Reaction tubes were incubated for 30 min at 37°C and 1 min at 70°C, and 30 μl of 1×TE (pH 8) were added to the reaction, which was then loaded on a MicroSpin G-25 Column (APBiotech), and spun down for 2 min to separate the labeled probe from unbound nucleotides. Labeled DNA probe (120 pg; ∼30,000 cpm) was incubated with 1 μg of bacterially expressed p53 in 20 μl buffer (12.5 mM Tris-HCl;pH 7.9, 25 mM KCl, 0.25 mM EDTA, 0.5 mM DTT and 5% glycerol). Where noted, 1 μl of PAb-421 ascites fluid was added. After incubation for 15 min at 4°C and 15 min at room temperature, the mixture was fractionated on a non-denaturing 4% acrylamide gel (37.5:1 acrylamide:bisacrylamide) in 0.4×TBE running buffer at 200 V for 1 h. Gels were dried under vacuum at 80°C for 45 min and autoradiographed overnight.

4.4 Sequencing of Idi-1 and Idi-2 variable regions

Total RNA was extracted from Idi-1 and Idi-2 hybridomas using TriReagent (Molecular Research Center, INC.), and the RNA was used as a template for cDNA synthesis using SuperScript Reverse Transcriptase (Invitrogen, Karlsruhe, Germany). PCR amplification of the heavy and light chain variable regions were performed using primers specific for the respective flanking constant region: 5′-CGGGAATTCCC-CAGGTGCAGCTGCAGCAGTCTGG and 3′-GCGGGCCCT-CGAGTCTATGTACATATGCAAGGCTTACAACC for the heavy chain; 5′-CGCGCAAGCTTGATATTGTGATAACCCAGGATGA and 3′-GATGGTGGGAAGATG for the light chain. PCR products were purified and sequenced using the same primers.

4.5 Molecular modeling

A structural model of the molecular complex of PAb-421 and Idi-1 was obtained by proceeding along the following steps: First, each antibody was modeled separately, based on structures of antibodies from the Protein Data Bank (PDB) [27]. Then the two antibodies were docked to obtain a model structure of the Fv-Fv complex. In the third step the conformations of side chains in the interacting CDR loops were manually modified to eliminate clashes and to optimize the interactions.

To model PAb-421 and Idi-1, the light and heavy chains of the Fv fragments were aligned with the sequences of antibodies whose experimental structures were available in the PDB. We found that the RNA recognizing antibody Fab fragment (PDB code 1mre) was an adequate template for modeling both the light and heavy chains of PAb-421; the sequences are similar, with 71% identity for the light chain and 72% identity for the heavy chain. The H3 loop model of PAb-421 was based on another antibody structure (PDB code 12e8), which has an H3 loop of the same length. The human monoclonal antibody Ctm01 (PDB code 1ad9) was used as a template for modeling Idi-1. Its sequence shows 54% identity to the light chain and 64% identity to the heavy chain of IDI-1. The H3 loops of 1ad9 and Idi-1 are the same length. Initial models were built using the Homology module of Insight II (Accelrys Inc., San Diego, CA). These were energy-minimized keeping the positions of Cα atoms fixed, except for the H3 loops, which do not have canonical structures [28].

Then, the two model structures were docked using the geometric-electrostatic version of the program MolFit [22]. This program uses digital three-dimensional representations of the molecules, which distinguish between their surface and interior, and searches for the best shape and electrostatic complementarity. The search is performed by rotating the molecules to different relative orientations and calculating the correlation matrix between their digital representations at the given orientation [29]. Good solutions have high correlation values (scores), which reflect good geometric and electrostatic complementarity. A full rotation/translation scan was performed with a translation grid interval of 1.13 Å and an angular interval of 12°. Interactions involving the portion of the Fv surface that normally connects to the Fc domain were prevented by defining them as ‘interior’. The electrostatic potential of each molecule was calculated using the program Delphi [30] as implemented in the MSI package. The scan produced 8,760 models, sorted by their geometric-electrostatic complementarity scores. The distribution of scores was analyzed by fitting it with an extreme-value distribution function [31]. This provided estimates of the mean score and the standard deviation. We manually analyzed the 50 best solutions by searching for solutions that mostly involved interactions between the CDR of the two antibodies. Four acceptable solutions were further refined by first eliminating small intermolecular clashes and then by allowing small 2° rotations about the position obtained in the scan.

Acknowledgements: This study was supported by the Minerva foundation and by grants from the Israel-USA Binational Science Foundation (BSF) the DIP (Deutsch-Israelische Projektkooperation) and the Kadoori Foundation.

I.R.C is the incumbent of the Mauerberger Chair in Immunology and V.R. is the incumbent of the Norman and Helen Asher Professorial Chair in Cancer Research at the Weizmann Institute.

References

1 **Hahn, B. H.,** Antibodies to DNA. *N. Engl. J. Med.* 1998. **338:** 1359–1368.

2 **Czaja, A. J., Morshed, S. A., Parveen, S. and Nishioka, M.,** Antibodies to single-stranded and double-stranded DNA in antinuclear antibody-positive type 1-autoimmune hepatitis. *Hepatology* 1997. **26:** 567–572.

3 **Pisetsky, D. S.,** The immunologic properties of DNA. *J. Immunol.* 1996. **156:** 421–423.

4 **Radic, M. Z. and Weigert, M.,** Genetic and structural evidence for antigen selection of anti-DNA antibodies. *Annu. Rev. Immunol.* 1994. **12:** 487–520.

5 **Herkel, J., Erez-Alon, N., Mimran, A., Wolkowicz, R., Harmelin, A., Ruiz, P., Rotter, V. and Cohen, I. R.,** Systemic lupus erythematosus in mice, spontaneous and induced, is associated with autoimmunity to the C-terminal domain of p53 that recognizes damaged DNA. *Eur. J. Immunol.* 2000. **30:** 977–984.

6 **Fields, B. A., Goldbaum, F. A., Ysern, X., Poljak, R. J. and Mariuzza, R. A.,** Molecular basis of antigen mimicry by an anti-idiotope. *Nature* 1995. **374:** 739–742.

7 **Goldbaum, F. A., Braden, B. C. and Poljak, R. J.,** The molecular basis of antigen mimicry by anti-idiotypic antibodies. *Immunologist* 1998. **6:** 13–18.

8 **Sharpless, N. E. and DePinho, R. A.,** p53: good cop/bad cop. *Cell* 2002. **110:** 9–12.

9 **Lee, S., Elenbaas, B., Levine, A. and Griffith, J.,** p53 and its 14 kDa C-terminal domain recognize primary DNA damage in the form of insertion/deletion mismatches. *Cell* 1995. **81:** 1013–1020.

10 **Reed, M., Woelker, B., Wang, P., Wang, Y., Anderson, M. E. and Tegtmeyer, P.,** The C-terminal domain of p53 recognizes DNA damaged by ionizing radiation. *Proc. Natl. Acad. Sci. USA* 1995. **92:** 9455–9459.

11 **Bakalkin, G., Selivanova, G., Yakovleva, T., Kiseleva, E., Kashuba, E., Magnusson, K. P., Szekely, L., Klein, G., Terenius, L. and Wiman, K. G.,** p53 binds single-stranded DNA ends through the C-terminal domain and internal DNA segments via the middle domain. *Nucleic Acids Res.* 1995. **23:** 362–369.

12 **Arai, N., Nomura, D., Yokota, K., Wolf, D., Brill, E., Shohat, O. and Rotter, V.,** Immunologically distinct p53 molecules generated by alternative splicing. *Mol. Cell Biol.* 1986. **6:** 3232–3239.

13 **Herkel, J., Mimran, A., Erez, N., Kam, N., Lohse, A. W., Marker-Hermann, E., Rotter, V. and Cohen, I. R.,** Autoimmunity to the p53 protein is a feature of systemic lupus erythematosus (SLE) related to anti-DNA antibodies. *J. Autoimmun.* 2001. **17:** 63–69.

14 **Herkel, J., Modrow, J. P., Bamberger, S., Kanzler, S., Rotter, V., Cohen, I. R. and Lohse, A. W.,** Prevalence of autoantibodies to the p53 protein in autoimmune hepatitis. *Autoimmunity* 2002. **35:** 493–496.

15 **Hylkema, M. N., van Bruggen, M. C., ten Hove, T., de Jong, J., Swaak, A. J., Berden, J. H. and Smeenk, R. J.,** Histone-containing immune complexes are to a large extent responsible for anti-dsDNA reactivity in the Farr assay of active SLE patients. *J. Autoimmun.* 2000. **14:** 159–168.

16 **Wolf, D., Harris, N., Goldfinger, N. and Rotter, V.,** Isolation of a full-length mouse cDNA clone coding for an immunologically distinct p53 molecule. *Mol. Cell Biol.* 1985. **5:** 127–132.

17 **Wolkowicz, R., Elkind, N. B., Ronen, D. and Rotter, V.,** The DNA binding activity of wild type p53 is modulated by blocking its various antigenic epitopes. *Oncogene* 1995. **10:** 1167–1174.

18 **Jang, Y. J. and Stollar, B. D.,** Anti-DNA antibodies: aspects of structure and pathogenicity. *Cell Mol. Life Sci.* 2003. **60:** 309–320.

19 **Tillman, D. M., Jou, N. T., Hill, R. J. and Marion, T. N.,** Both IgM and IgG anti-DNA antibodies are the products of clonally selective B cell stimulation in (NZB x NZW)F1 mice. *J. Exp. Med..* 1992. **176:** 761–779.

20 **Krishnan, M. R., Jou, N. T. and Marion, T. N.,** Correlation between the amino acid position of arginine in VH-CDR3 and specificity for native DNA among autoimmune antibodies. *J. Immunol.* 1996. **157:** 2430–2439.

21 **Barry, M. M., Mol, C. D., Anderson, W. F. and Lee, J. S.,** Sequencing and modeling of anti-DNA immunoglobulin Fv domains. Comparison with crystal structures. *J. Biol. Chem.* 1994. **269:** 3623–3632.

22 **Heifetz, A., Katchalski-Katzir, E. and Eisenstein, M.,** Electrostatics in protein-protein docking. *Protein Sci.* 2002. **11:** 571–587.

23 **Mendez, R., Leplae, R., De Maria, L. and Wodak, S. J.,** Assessment of blind predictions of protein-protein interactions: current status of docking methods. *Proteins* 2003. **52:** 51–67.

24 **Rustandi, R. R., Baldisseri, D. M. and Weber, D. J.,** Structure of the negative regulatory domain of p53 bound to S100B(betabeta). *Nat. Struct. Biol.* 2000. **7:** 570–574.

25 **Burlingame, R. W., Boey, M. L., Starkebaum, G. and Rubin, R. L.,** The central role of chromatin in autoimmune responses to histones and DNA in systemic lupus erythematosus. *J. Clin. Invest.* 1994. **94:** 184–192.

26 **DeLeo, A. B., Jay, G., Appella, E., Dubois, G. C., Law, L. W. and Old, L. J.,** Detection of a transformation-related antigen in chemically induced sarcomas and other transformed cells of the mouse. *Proc. Natl. Acad. Sci. USA* 1979. **76:** 2420–2424.

27 **Berman, H. M., Westbrook, J., Feng, Z., Gilliland, G., Bhat, T. N., Weissig, H., Shindyalov, I. N. and Bourne, P. E.,** The Protein Data Bank. *Nucleic Acids Res.* 2000. **28:** 235–242.

28 **Chothia, C., Lesk, A. M., Tramontano, A., Levitt, M., Smith-Gill, S. J., Air, G., Sheriff, S., Padlan, E. A., Davies, D., Tulip, W. R., Colman, P. M., Spinelli, S., Alzari, P. M. and Poljak, R. J.,** Conformations of immunoglobulin hypervariable regions. *Nature* 1989. **342:** 877–883.

29 **Katchalski-Katzir, E., Shariv, I., Eisenstein, M., Friesem, A. A., Aflalo, C. and Vakser, I. A.,** Molecular surface recognition: determination of geometric fit between proteins and their ligands by correlation techniques. *Proc. Natl. Acad. Sci. USA* 1992. **89:** 2195–2199.

30 **Honig, B. and Nicholls, A.,** Classical electrostatics in biology and chemistry. *Science* 1995. **268:** 1144–1149.

31 **Levitt, M. and Gerstein, M.,** A unified statistical framework for sequence comparison and structure comparison. *Proc. Natl. Acad. Sci. USA* 1998. **95:** 5913–5920.

Correspondence: Irun R. Cohen, The Department of Immunology, The Weizmann Institute of Science, 76100 Rehovot, Israel
Fax: +972-8-934-4103
e-mail: Irun.Cohen@weizmann.ac.il

